BS 2021 1-3 SEPT BRUGES
INTERNATIONAL BUILDING PERFORMANCE SIMULATION ASSOCIATION

Investigating the control strategies for Breathing Walls during summer: a dynamic simulation study

Andrea Alongi[1], Adriana Angelotti[1], Livio Mazzarella[1]
[1]Politecnico di Milano, Milano, Italy

Abstract

The paper aims at studying different strategies for the optimal operation of Breathing Walls during summer. The investigation is carried out by performing dynamic simulations on a case study. To this purpose, a transient Finite-Difference numerical model for Breathing Wall components, previously developed in Matlab and validated by the Authors, is coupled with TRNSYS. The case study consists of an office room located in Milan, Italy, provided with Air Conditioning and Mechanical Ventilation and with an air permeable wall. Forcing exhaust air from the indoor environment across the Breathing Wall has better performances compared to forcing supply air from the outside across the wall. Yet modest energy savings are found compared to the traditional impermeable use of the wall, as the high level of insulation already minimises the heat gains through the opaque envelope.

Key Innovations

- Breathing Wall model coupled to a Building Energy Simulation tool
- Dynamic simulations of summer behaviour in North Mediterranean climate
- Impact of the air flow direction across the BW critically discussed
- Control strategy for day and night operation of the BW identified

Practical Implications

Always perform a building dynamic simulation to understand any advantage of summer use of a Breathing Wall; a control strategy for the air flow direction needs to be designed; if the opaque envelope is well insulated the pros of the Breathing Wall in summer are found to be limited.

Introduction

Breathing Walls (BW) are made of porous materials that can be permeated by a forced or naturally driven airflow. They have been firstly proposed in countries where heating demand is dominating, as a mean to pre-heat the ventilation air from the outdoor environment by recovering the heat losses across the walls (Taylor et al. 1996). In these contexts, BWs feature porous insulation materials (e.g. mineral wool).

Conversely, the optimal use of BWs in the cooling season still needs to be explored: some Authors (Zhang et al. 2019) suggested the so-called Exhaust Air Insulation mode, namely forcing exhaust air from the conditioned indoor environment across the BW to reduce the envelope heat gains. They report a significant difference between the hourly heat gain of the wall with and without exfiltration airflow, although in their model the indoor environment is summarised as a boundary condition and thus the weight of the wall heat gain in the indoor energy balance is not assessed. In (Ascione et al. 2017) it is proposed to couple a cellulose-based BW with night free cooling, by forcing the outdoor fresh air introduced into the building across the permeable wall. It is shown that the cooling of the wall is quite faster compared to traditional night free cooling. However, it has to be remarked that the analysis assumes a uniform initial temperature equal to 40°C inside the wall, as a result of solar irradiation during the day.

To summarise, previous studies concerning the use of BWs during summer either limit the boundary of the analysis to the wall or assume simplified conditions inside it. A comprehensive dynamic simulation of a building zone featuring a permeable envelope, considering the dynamic of the summer weather conditions and of the indoor gains during day and night, is still lacking.

To this purpose in this paper for the first time a numerical model previously developed for BW components by the Authors (Alongi et al. 2021) is integrated with an existing Building Energy Simulation tool, namely TRNSYS.

The integrated model is used to give insights into the summer use of this technology in the Northern Italy climatic context for an office building application. The two airflow directions across the BW are considered, as well as the coupling with free cooling during the night, in order to assess an optimal control strategy.

Methodology

In this work the effects of the air velocity through the porous layers of a BW are assessed calculating the overall cooling energy need of a virtual case study modeled in TRNSYS 18.

https://doi.org/10.26868/25222708.2021.30519

The Breathing Wall numerical model

The thermal behavior of an air-permeable layer inside a Breathing Wall component is represented by a modified Fourier equation, expressed as:

$$(\rho c)_w \frac{\partial T}{\partial t} + u_f (\rho c_p)_f \frac{\partial T}{\partial x} = \lambda_w \frac{\partial^2 T}{\partial x^2} \quad (1)$$

where T is the temperature inside the domain, assumed as a function of time t and space x, u_f is the airflow velocity across the wall (positive when the air moves from the outdoor to the indoor environment, negative when the air is exhausted through the wall, null when the layer acts as a non-permeable one) and ρ, c and λ are the density, the specific heat (at constant pressure if p subscript is indicated) and the thermal conductivity of porous material (subscript w) or air (subscript f). Eq. (1) is also based on the hypothesis of constant thermal-physical properties of the material and local thermal equilibrium (Kaviany, 1995; Alongi and Mazzarella, 2015). This allows to neglect microscopic thermal interactions between the solid and the fluid phase and to calculate the volume weighted average thermal-physical properties of the porous material.

In order to simulate the thermal behavior of a BW, a Finite Difference Model, based on Eq. (1), has been developed and validated, as presented in (Alongi et al. 2021), through direct comparison with the exact solution of the steady periodic problem described in (Alongi et al. 2020). This model is full implicit in time and approximates both spatial derivatives in the diffusion-advection equation using the central difference scheme (second order for the diffusive term and first order for the advective one). According to the outcomes of the validation work, it is possible to set here the spatial and time discretization to 0.001 m and 0.25 h respectively. In this way it is possible to maximize the accuracy without a significant increase in computational cost.

The algorithm is written in Matlab language and is able to manage multi-layer domains, considering both permeable and non-permeable materials through the numerical scheme mentioned above. Moreover, it is possible to consider ventilated and non-ventilated cavities. The convective part of the heat exchange is managed assuming a constant Nusselt number equal to 4.86 (Incropera, 2011) in the former, while the latter is treated using the indications reported in the technical standard ISO 6946:2017. It is important to highlight that the assumption made for the ventilated cavity is due to the lack for reliable references from literature dedicated to BW technologies. Future work will be dedicated to improve on this aspect. The radiative component of the heat transfer is calculated in both cases using the linearization of the radiative problem. Since the overall convective-radiative coefficient of cavities depends on surface temperatures, the non-linearity of the physical problem is dealt with an iterative process. Convergence is reached when temperature residuals are below 10^{-3} °C in the whole domain. Both on the indoor and outdoor surface of the wall Robin boundary conditions are imposed, along with an imposed heat flux on the outdoor to keep into consideration solar radiation.

Finally, the boundary conditions for the heat transfer differential problem under discussion are defined using the finite volume method: for every geometrical discontinuity (external and internal surface, interface between adjacent layers), the energy balance for a reference volume is defined.

Coupling the BW model with TRNSYS

The Matlab Finite Difference Model is linked to the Multi-Zone Building model type 56 available in TRNSYS 18 through the type 155 (Calling External Programs - Matlab).

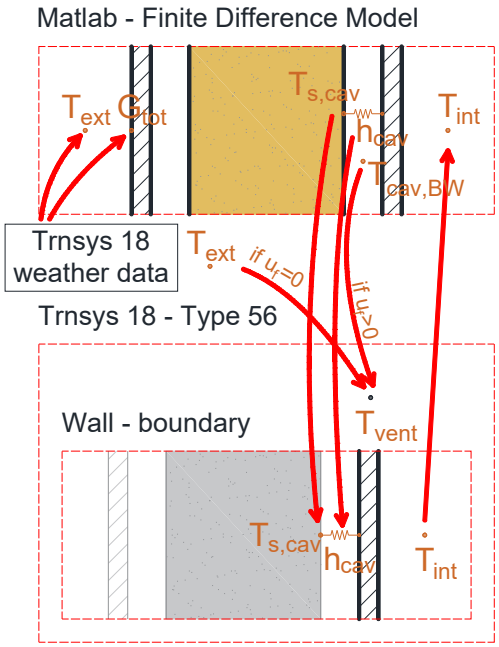

Figure 1: BW modelling and coupling between the Matlab algorithm and type 56 (TRNSYS 18)

The link between the wall and the building model is achieved using a recursive approach (Figure 1). Inside the Multi-Zone Building model, only the innermost impermeable layer of the BW is defined and is set as a boundary surface, allowing the user to define both an outdoor temperature and the outside surface heat transfer coefficient. At the same time, the Matlab algorithm provides three outputs: the convective-radiative heat transfer coefficient and the temperature of the outer surface of the innermost cavity (h_{cav} and $T_{s,cav}$ in Figure 1), either ventilated or not, and the average air temperature of the internal ventilated cavity ($T_{cav,BW}$).

h_{cav} and $T_{s,cav}$ are used by the building model as input to solve the boundary surface (namely the BW) conductive balance, while $T_{cav,BW}$ is used as ventilation air temperature, whenever the air flows inward through the permeable envelope. On the contrary, if the external wall is not permeable or the air is exhausted through it, the ventilation air temperature is assumed equal to the outdoor one, meaning that the external air is directly

https://doi.org/10.26868/25222708.2021.30519

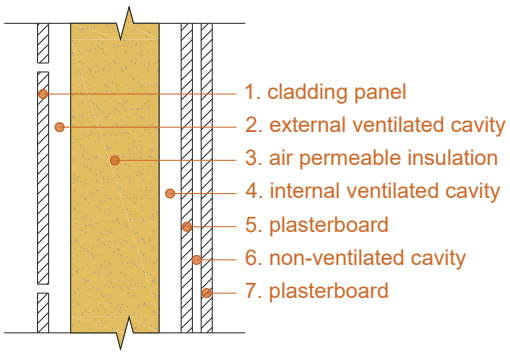

Figure 2: wall layer sequence.

Table 1: thickness and physical properties of the layers inside the external wall.

ID	s [m]	λ [W/(mK)]	ρ [kg/m³]	c [J/(kgK)]
1	0.025	0.35	1150	1000
2	0.05	-	-	-
3	0.20	0.034	50	1030
4	0.05	-	-	-
5	0.025	0.25	1000	1000
6	0.02	-	-	-
7	0.025	0.25	1000	1000

Table 2: summary of main simulations settings.

ID	wall technology	wall airflow		Ventilation	
		day	night	day	night
1.0 (ref.)	traditional	-	-	1.59 h^{-1}	-
1.1	Breathing Wall	inward	-	1.59 h^{-1}	-
1.2	Breathing Wall	outward	-	1.59 h^{-1}	-
1.3	Breathing Wall	outward (if $T_{se}>T_{air,\,int}$)	-	1.59 h^{-1}	-
2.0 (ref.)	traditional	-	-	1.59 h^{-1}	1.59 h^{-1}
2.1	Breathing Wall	outward (if $T_{se}>T_{int}$)	outward (if $T_{ext}<T_{int}$)	1.59 h^{-1}	1.59 h^{-1}
2.2	Breathing Wall	outward (if $T_{se}>T_{int}$)	-	1.59 h^{-1}	1.59 h^{-1}
3.0 (ref.)	traditional	-	-	1.59 h^{-1}	10 h^{-1}
3.1	Breathing Wall	outward (if $T_{se}>T_{int}$)	outward (if $T_{ext}<T_{int}$)	1.59 h^{-1}	10 h^{-1}
3.2	Breathing Wall	outward (if $T_{se}>T_{int}$)	-	1.59 h^{-1}	10 h^{-1}

supplied to the indoor environment. Then, with the hypothesis of perfect mixing, it is expelled either through a ventilation opening (traditional wall case) or through the air permeable wall (BW case).

As far as the differential problem is concerned, the boundary conditions for the Finite Difference algorithm are provided at every timestep by the weather data reader for the outdoor edge (air temperature and total incident radiation) and by the building model for the indoor surface (zone air temperature), providing a closure to the recursive problem.

Going more in detail about the indoor boundary condition, since at this stage the Finite Difference model is not able to deal separately with convective and radiative heat transfer, it is not possible to use the standard radiation mode (starnet model), which is substituted by the one node model.

The case study

The virtual case study consists of a single thermal zone representing a two-occupants office modeled on the basis of the small-size office modules inside the Energy Department building of Politecnico di Milano (Italy).

This model has a floor area of 16.6 m^2, an inter-storey height of 3 m and a volume of 49.81 m^3. The external surfaces consist of a 3.69 m^2 window and a 10.11 m^2 opaque wall, both with South exposition. The wall, as represented in Figure 2, features the following layer sequence: an external cladding as rain protection, an external ventilated air cavity, an insulating air permeable layer (which works as BW element), an internal ventilated air cavity, a first plasterboard, an internal non-ventilated air cavity (dedicated to the installation of electrical connections) and a final plasterboard. Layer properties are reported in Table 1.

The zone is occupied by two persons during working hours (from 9:00 to 13:00 and from 14:00 to 18:00). During occupation internal gains are set to 20 W/m^2, taking into account all components (i.e. people, PCs, lights, etc.), and to a base value of 2 W/m^2 during the rest of the day, to take into account for stand-by of electronic equipment. The number of people is also used to define the airchange rate for the ventilation system, which is based on the prescription of the (UNI 10339:1995) requiring $11 \cdot 10^{-3}$ m^3/s per person. This leads to a base airchange (ACH) rate (n_{day}) of 1.59 h^{-1}, corresponding to an airflow velocity through the BW of around 0.0022 m/s,

whenever this technology is simulated. This value is calculated dividing the volumetric airflow rate by the net external wall area. Finally, the cooling system (AC) is considered active from 6:00 to 18:00, when the set-point (T_{sp}) is assumed 26 °C. The same schedule is used also to activate the ventilation system, whenever the night free-cooling is not implemented.

Simulations are run from May to September with 0.25 h time step using Milan weather files.

The analyses are performed in two main steps: in the first, ventilation is active only during daytime and the two main working regimes for BW (airflow directed inward and outward alternatively) are compared to a reference non permeable case. The second set of simulations features the implementation of free-cooling during the night and is focused on the behavior of the BW crossed by exhaust air from indoor. Table 2 summarizes the main simulation settings adopted.

Results and Discussion

The first group of simulations (identified as 1.0-1.3) is aimed at evaluating the two main working regimes for BW technology against a traditional wall (non-permeable) with the same layer sequence, which is used as a reference. The BW simulations are therefore performed with airflow directed inward ($u_f>0$) and outward ($u_f<0$) alternatively, both during the AC working time i.e. from 6:00 to 18:00. As it was mentioned in the Introduction, in literature the first working regime is typically adopted in winter conditions, while the second is theoretically more suitable for summer conditions. It is important to notice that the comparison is not performed in terms of electrical energy need, with the inclusion of auxiliary consumptions (i.e. fans), but is limited to the thermal energy need. Even though it is possible to imagine a local ventilation system where the BW technology is implemented and calculate its consumptions, an Air Handling Unit (AHU) is typically adopted in traditional plants and serves the whole building. Therefore, it would have been difficult to properly estimate the fraction of electrical energy absorbed by the AHU to provide airchanges to the simulated zone, hence missing a reliable reference. This kind of analysis will be performed in the future, when a whole building will be investigated.

The outcomes of this first set of simulations are reported in Table 3, where the maximum cooling power and the seasonal cooling energy need are presented.

The results reported in Table 3 for simulation 1.1 confirm that introducing the air into the room by passing it through the wall is not convenient, since it leads to a rise in both energy demand and maximum cooling power requirement. This happens because, overall, the energy provided by the solar radiation incident on the outer surface is transported inward by the airflow, heating up the wall and causing a rise in the ventilation air temperature.

On the other hand, exhausting the air through the wall (simulation 1.2 in Table 2 and Table 3) has two opposite effects: a slight reduction in peak load (-1.3 %) and a very small increase in cooling energy demand (+0.6 %). A deeper investigation of the simulation results in comparison with the reference ones is thus needed.

In Figure 3 the daily cooling energy need during the month of August is reported for the reference simulation with the traditional non-permeable technology (1.0) and that dealing with a Breathing Wall component working as exhaust element (1.2). It is possible to observe that the two series of data present comparable values. However, whenever the daily energy need is higher (above 6-7 kWh/day) the BW component is more convenient, while the opposite happens when the energy need is smaller. Results are further investigated in two representative days of the month. More in detail, the cooling load is compared to the advective heat flux through the wall, defined as:

$$\dot{Q}_{adv,BW} = A_{BW}|u_f|(\rho c_p)_f(T_{se} - T_{air,int}) \qquad (2)$$

where A_{BW} is the frontal area of the Breathing Wall, T_{se} is the external surface temperature and $T_{air,int}$ is the indoor air temperature. Eq. (2) gives the heat rate gained by the airflow through the wall, which is positive when the air is heated when crossing the wall, that is in turn cooled with a positive effect on the overall zone balance. Conversely, negative values are averse to the cooling energy need reduction and must be minimized.

Figure 4 shows the trend of the cooling load and of the advective flux through the BW in two days with opposite outcomes. August 6th features a better performance registered for the BW technology than for the traditional one. Indeed, it is possible to observe that the cooling demand is comparable to the advective heat flux during the day. However, from hour 6 to 9 the advective flux is negative and therefore detrimental. Integration during the day shows that, even though non prevalent, the negative contribution calculated during the early morning hours (-228.4 Wh) significantly reduces positive effects of the technology (from 2023.7 Wh to 1795.3 Wh). The same happens during the August 28th, when the overall energy need is lower for both technologies investigated, with a slight advantage for the traditional one.

However, in this case the negative part of the advective flux is more relevant and happens during two different periods of the day (from 6 to 11 and from 17 to 18), leading to an integral value of -641.0 Wh, which is more significant than the positive one of 382.6 Wh, achieved during the period from hour 11 to 17. This results on a negative daily integral of -258.5 Wh, that worsens the performance compared to the traditional technology.

https://doi.org/10.26868/25222708.2021.30519

Table 3: simulations comparing non-permeable and permeable modes during daytime.

ID	technology	wall airflow	Q'_{max}		Q_{tot}	
			[W]	Δ to ref.	[kWh]	Δ to ref.
1.0 (ref.)	traditional	none	1110.3	-	767.0	-
1.1	Breathing Wall	inward	1241.5	11.8 %	867.5	13.1 %
1.2	Breathing Wall	outward	1095.9	-1.3 %	771.5	0.6 %
1.3	Breathing Wall	outward (if $T_{se}>T_{air,\,int}$)	1095.8	-1.3 %	764.2	-0.4 %

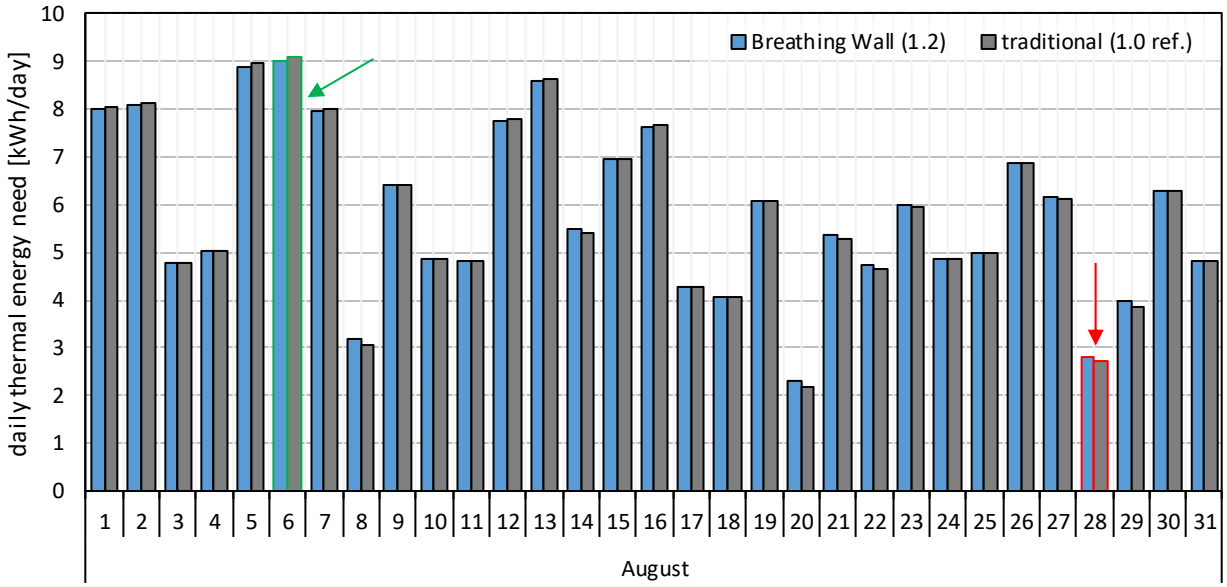

Figure 3: Daily cooling energy need in August in cases 1.0 and 1.2.

This analysis, along with Eq. (2), suggests to implement a control strategy for a hypothetical ventilation system linked to a BW component, in order to decide, at any given time, if it is more convenient to expel the air through the wall or directly outside during the daytime. Therefore it is set that the airflow crosses the wall when $T_{se}>T_{air,int}$, while it is expelled directly outside otherwise. This strategy is applied in a new simulation (ID: 1.3), performed with the other settings inherited from simulation 1.2. Its results (Table 3) show the same requirement in maximum cooling power (1095.8 W), while the energy need is slightly reduced to 764.2 kWh. Even though the improvement is modest, the trend demonstrates that the control strategy is effective.

At this point, it is possible to draw few conclusions from this first set of analyses: first of all, when the ventilation system is active only during daytime simultaneously to the cooling system, it is more convenient to use the Breathing Wall as an exhaust element, rather than a supply one. Moreover, it proves to be useful to deactivate the airflow through the envelope whenever indoor air temperature is above the external surface one, instantaneously switching to a traditional approach. However, due to the low thermal transmittance of the external wall and to the small activation time range, deviations from the reference condition are marginal, since heat gains through the opaque part of the envelope are already contained. As an example, Table 4 reports the main components of the thermal zone energy balance in two reference days: the cooling load managed by the AC (Q_{cool}), along with the loads due to ventilation (Q_{vent}), heat transfer through the envelope (Q_{trans}), internal ($Q_{g,int}$) and solar (Q_{sol}) gains. It shows that the improvement is achieved by maximizing the energy expelled through conduction. However, this term is significantly smaller than the internal and solar gains that cause most of the cooling load.

For this last reason, a new set of simulations (ID: 2.0,2.1,3.0,3.1 in Table 2) is performed where free-cooling is implemented during the night, (namely, from 18 to 6, when the AC is not active) with two levels of airchange rates. The first one maintains the same value assumed during daytime operation (1.59 h^{-1}), while the second one is increased up to 10 h^{-1} (n_{night}), to maximize the contribution of the ventilation term in the thermal zone energy balance. As far as BW operation is concerned, only airflow directed outward is considered, since it appears to be the more promising approach for summer conditions, and the control strategy previously discussed is implemented for daytime operation. The increased airchange rate rises the airflow through the BW to 0.0137 m/s. Moreover, during night the ventilation system is activated only when external air temperature is lower than the indoor one.

Results are summarized in Table 5, again in terms of maximum cooling load and cooling energy need during summer season. First, it is possible to note that the implementation of the free-cooling during the night provides a significant reduction of the seasonal energy

https://doi.org/10.26868/25222708.2021.30519

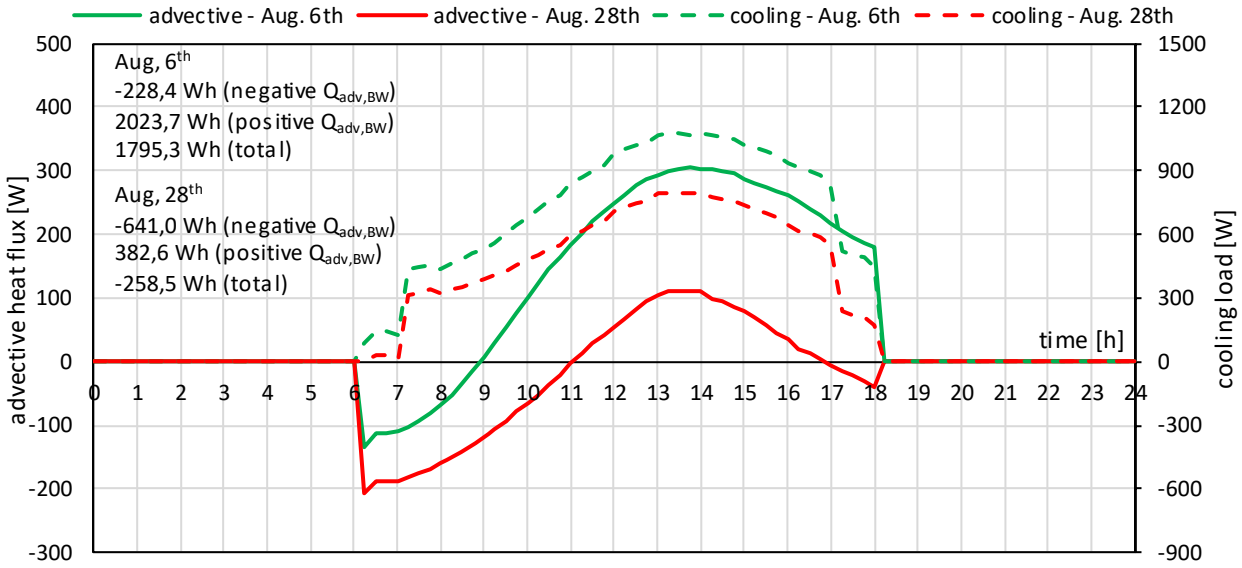

Figure 4: Cooling load (right axis) and advective flux through the BW (left axis) in case 1.2 in two representative days.

Table 4: main components of the daily energy balance for the thermal zones in two representative days.

	Aug, 6th					*Aug, 28th*				
	Q_{cool} [kWh]	Q_{vent} [kWh]	Q_{trans} [kWh]	$Q_{g,int}$ [kWh]	Q_{sol} [kWh]	Q_{cool} [kWh]	Q_{vent} [kWh]	Q_{trans} [kWh]	$Q_{g,int}$ [kWh]	Q_{sol} [kWh]
traditional (1.0 ref.)	8.96	0.82	-0.26	3.78	4.62	6.11	-1.14	-0.48	3.78	3.94
Breathing Wall (1.2)	8.89	0.82	-0.33	3.78	4.62	6.14	-1.14	-0.44	3.78	3.94
Breathing Wall (1.3)	8.87	0.82	-0.36	3.78	4.62	6.09	-1.14	-0.49	3.78	3.94

demand, going from 767 kWh to 511 kWh (ACH = 1.59) or 283 kWh (ACH = 10) for the traditional technologies.

Like in the results observed in the first set of analyses (1.3 versus 1.0), the difference between a traditional approach and the implementation of BW technology is small in both night airflow rates considered. Again, it is possible to note that using the wall as the exhaust element of the ventilation system leads to a slight mitigation of the peak in cooling load. However, its effect on the seasonal energy need is detrimental in simulation 2.1 (compared to simulation 2.0), while a minimal improvement is observed for simulation 3.1 (with simulation 3.0 as reference). The Authors' opinion is that this small overall effect of the BW is related to the properties of the external wall, which features a high thermal resistance and a low thermal capacity, leading to a negligible ability to store thermal energy during the day and release it during night.

It is possible to infer that a more capacitive solution might benefit more from the airflow exhausted through the air permeable layers. However, this hypothesis will be further investigated in the future.

An in depth analysis on a significant summer day (August 6th) is performed, by evaluating the internal energy of the wall at every timestamp for all the simulations reported in Table 5, using the temperature distribution returned by the Matlab algorithm (Figure 5).

Taking into account that lower levels of internal energy correspond to a better thermal performance of the wall in summer conditions (i.e. lower temperatures across the wall section), it is possible to divide the curves reported in Figure 5 into three main regions. In the time frame from 6 to 18 (when airchange rates are set to 1.59 h^{-1} in all cases), there is generally an advantage for the BW, with the only exclusion of the very first part of this range, when the control strategy discussed previously is active and in all the simulations the wall is not crossed by air. The effect of a higher airchange rate during night consists of more effective structures discharge and reduction of the load on the AC plant. The time frame from 18 to 23 is characterized by small differences among all curves: this is due to the effect of the control strategy applied to the night ventilation, which is switched off whenever outdoor air temperature is higher than the indoor one. The third period is finally identifiable from 23 to 6, when the night ventilation is active. During this period, the traditional approach has a slight advantage over the BW one at both airflow levels, meaning that the airflow through the permeable wall is partially charging the structures from the inside, due to the internal gains and the solar gains that have entered the window the day before.

Table 5: simulations comparing the effects of night-time free cooling, with two levels of airchange rates, on non-permeable and permeable modes.

ID	technology	n_{day} [h^{-1}]	n_{night} [h^{-1}]	Q'_{max} [W]	Δ to ref.	Q_{tot} [kWh]	Δ to ref.
2.0 (ref.)	traditional	1.59	1.59	1059.9		511.4	
2.1	Breathing Wall	1.59	1.59	1046.2	-1.3%	518.6	1.4%
2.2	Breathing Wall	1.59	1.59	1044.0	-1.5%	508.5	-0.7%
3.0 (ref.)	traditional	1.59	10	955.7		282.6	
3.1	Breathing Wall	1.59	10	940.2	-1.6%	280.4	-0.8%
3.2	Breathing Wall	1.59	10	939.5	-1.7%	279.4	-1.3%

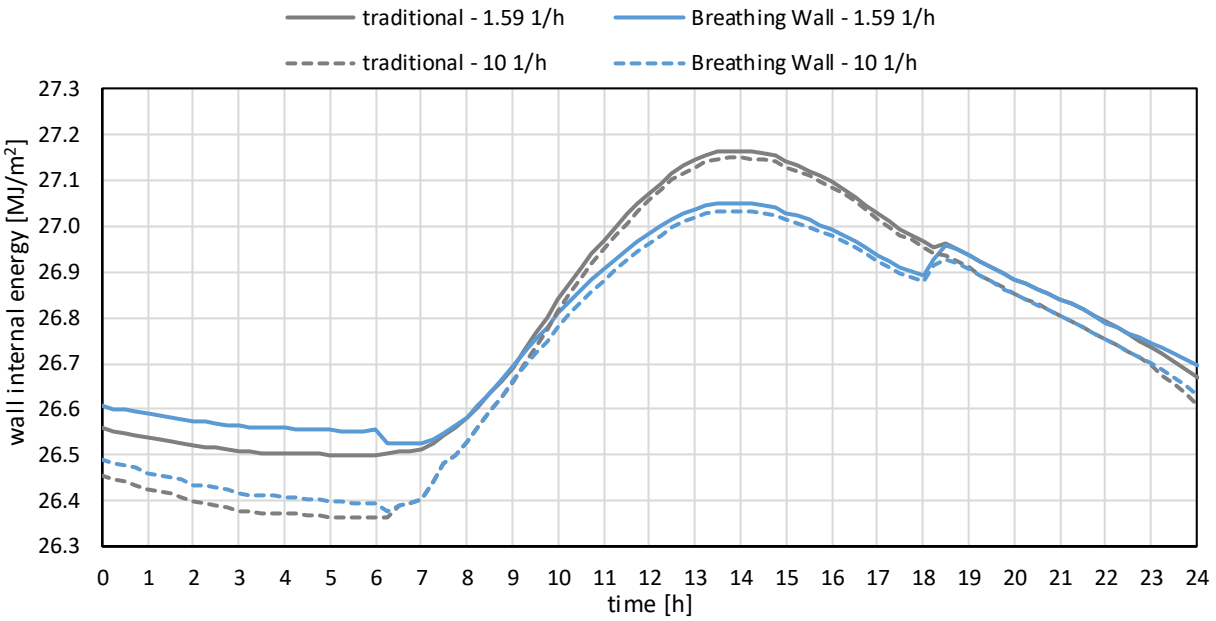

Figure 5: Internal energy variation inside the envelope during a representative day for non-permeable (traditional) and permeable (Breathing Wall) modes.

This analysis leads to a hybrid approach: the external wall is crossed by the airflow during daytime, whenever the outer surface temperature is higher than the indoor air temperature, while during night time the system switches to a traditional behavior and the ventilation air is exhausted directly to the outdoor environment.

This control strategy has been tested through a new simulation for each free cooling airchange rate (ID: 2.2 and 3.2) and in Table 5 shows a small improvement over the previous approach: at 1.59 h^{-1} the peak load and the seasonal energy need become 1044 W and 508 kWh (-0.7 %) respectively, while at 10 h^{-1} these two quantities become 939 W and 279 kWh (-1.3 %). Again, the properties of the envelope seem to limit the ability of the advective heat flux to enhance the dissipation of the heat stored by the structures, due to its lack of thermal capacity. This implies that all the terms of the zone energy balance that constitute a load for the AC system are rapidly passed from the masses to the internal air.

Conclusion

The comprehensive BW and building simulation allowed to verify that, although in principle exhaust air from the indoor environment passing through the permeable walls reduces the heat gains, the benefits in terms of the cooling energy demand are marginal whenever:

i) the opaque envelope is well insulated, so that the heat gains through it are small and the wall temperature increases marginally during the day;
ii) the zone cooling load is dominated by the internal gains and the windows solar gains and the walls thermal capacity is insufficient to efficiently store them.

These considerations apply both during daytime, when the air from the indoor environment crossing the BW is maintained at the set point temperature by the Air Conditioning system, and night-time, when outdoor ventilation air is exhausted through the BW.

Moreover, it was highlighted that the indoor exhaust air can be warmer than the BW in the early morning, so that a control system is necessary to activate the airflow through the permeable envelope only when it would actually cool the wall.

Therefore, in the conditions studied in this paper, using BW during summer is not advantageous. Since in climates dominated by the cooling need less insulated and more capacitive walls are traditionally adopted, future developments will address the convenience of summer

https://doi.org/10.26868/25222708.2021.30519

operation of BW in those conditions. Furthermore, in climates where both heating and cooling are important, a different approach to building envelope design will be tested. Since in the contra-flux mode the effective thermal resistance of the BW becomes larger than the corresponding traditional wall (Taylor and Imbabi, 1998), the design thermal resistance can be achieved with either a traditional wall with an insulation thickness *s* or with a BW crossed by the required ventilation airflow, yet featuring a smaller insulation thickness *s'*. This way the wall stratigraphy could be designed to include also a porous capacitive layer toward the indoor. Following this approach, the overall year performance will be taken into consideration, in order to find design guidelines to balance and maximize both the winter and summer performance of the system.

References

Alongi A., Mazzarella L. (2015). Characterization of fibrous insulating materials in their application in dynamic insulation technology. Energy Procedia (78) 537-542.

Alongi A., Angelotti A. and Mazzarella L. (2021). A numerical model to simulate the dynamic performance of Breathing Walls, Journal of Building Performance Simulation, 14:2, 155-180, DOI: 10.1080/19401493.2020.1868578.

Alongi A., Angelotti A. and Mazzarella L. (2020). Experimental Validation of a Steady Periodic Analytical Model for Breathing Walls, Building and Environment 168: 106509. doi:10.1016/j.buildenv.2019.106509.

Ascione, F, Bianco N. and De Stasio C. (2015). Dynamic insulation of the building envelope: numerical modelling under transient conditions and coupling with nocturnal free cooling. Applied Thermal Engineering 84, 1–14.

Ente Nazionale Italiano di Unificazione (1995). Impianti aeraulici al fini di benessere. Generalità, classificazione e requisiti. Regole per la richiesta d'offerta, l'offerta, l'ordine e la fornitura (UNI 10339:1995).

Incropera F.P., Dewitt D.P. (2011). Fundamentals of Heat and Mass Transfer, 7th Edition, Wiley Ed., Hoboken (USA), p. 553.

International Organisation for Standardisation (2017). Building components and building elements – Thermal resistance and thermal transmittance – Calculation methods (ISO 6946:2017).

Kaviany M. (1995). Principle of Heat Transfer in Porous Media - second edition. Springer New York

Taylor B.J., Cathworne D.A., Imbabi M.S. (1996). Analytical Investigation of the Steady-State Behaviour of Dynamic and Diffusive Building Envelopes. Building and Environment 31 (6), 519-525.

Taylor B.J., Imbabi M.S. (1998). The application of Dynamic Insulation in buildings. Renewable Energy 15, 377-382.

Zhang, C., Wang J., Li L., Gang W. (2019). Dynamic thermal performance and parametric analysis of a heat recovery building envelope based on air-permeable porous materials. Energy 189, 116361.